Developmental and Comparative Immunology 79 (2018) 128–136

Contents lists available at ScienceDirect

Developmental and Comparative Immunology

journal homepage: www.elsevier.com/locate/dci

A conserved Toll-like receptor-to-NF-κB signaling pathway in the endangered coral *Orbicella faveolata*

Leah M. Williams [a], Lauren E. Fuess [b], Joseph J. Brennan [a], Katelyn M. Mansfield [a], Erick Salas-Rodriguez [a], Julianne Welsh [a], Jake Awtry [c], Sarah Banic [c], Cecilia Chacko [c], Aarthia Chezian [c], Donovan Dowers [c], Felicia Estrada [c], Yu-Hsuan Hsieh [c], Jiawen Kang [c], Wanwen Li [c], Zoe Malchiodi [c], John Malinowski [c], Sean Matuszak [c], Thomas McTigue IV [c], David Mueller [c], Brian Nguyen [c], Michelle Nguyen [c], Phuong Nguyen [c], Sinead Nguyen [c], Ndidi Njoku [c], Khusbu Patel [c], William Pellegrini [c], Tessa Pliakas [c], Deena Qadir [c], Emma Ryan [c], Alex Schiffer [c], Amber Thiel [c], Sarah A. Yunes [c], Kathryn E. Spilios [c], Jorge H. Pinzón C [b], Laura D. Mydlarz [b], Thomas D. Gilmore [a, *]

[a] Department of Biology, Boston University, Boston, MA 02215, USA
[b] Department of Biology, University of Texas at Arlington, Arlington, TX 76019, USA
[c] Molecular Biology Laboratory (BB522), Program in Biochemistry & Molecular Biology, Boston University, Boston, MA 02215, USA

ARTICLE INFO

Article history:
Received 16 September 2017
Received in revised form
23 October 2017
Accepted 24 October 2017
Available online 26 October 2017

Keywords:
NF-kappaB
Toll-like receptor
Evolution
Coral
Innate immunity
Orbicella faveolata

ABSTRACT

Herein, we characterize the Toll-like receptor (TLR)-to-NF-κB innate immune pathway of *Orbicella faveolata* (Of), which is an ecologically important, disease-susceptible, reef-building coral. As compared to human TLRs, the intracellular TIR domain of Of-TLR is most similar to TLR4, and it can interact *in vitro* with the human TLR4 adapter MYD88. Treatment of *O. faveolata* tissue with lipopolysaccharide, a ligand for mammalian TLR4, resulted in gene expression changes consistent with NF-κB pathway mobilization. Biochemical and cell-based assays revealed that Of-NF-κB resembles the mammalian non-canonical NF-κB protein p100 in that C-terminal truncation results in translocation of Of-NF-κB to the nucleus and increases its DNA-binding and transcriptional activation activities. Moreover, human IκB kinase (IKK) and Of-IKK can both phosphorylate conserved residues in Of-NF-κB *in vitro* and induce C-terminal processing of Of-NF-κB *in vivo*. These results are the first characterization of TLR-to-NF-κB signaling proteins in an endangered coral, and suggest that these corals have conserved innate immune pathways.

1. Introduction

The Toll-like receptor (TLR)-to-NF-κB signaling pathway is a prominent innate immune pathway in higher metazoans. Specific pathogen-associated molecular patterns (PAMPs) are detected by membrane-bound TLRs, which then initiate intracellular signaling cascades. One main TLR pathway leads to activation of transcription factor NF-κB to induce changes in the expression of genes encoding innate immune effector molecules such as cytokines and anti-microbial peptides (Akira et al., 2006; Kawai and Akira, 2007). TLR-to-NF-κB pathways have been intensively studied for their roles in immunity in many model systems from flies to humans (Aderem and Ulevitch, 2000; Kawai and Akira, 2007; Minakhina and Steward, 2006; Silverman and Maniatis, 2001; Vasselon and Detmers, 2002). Recently, genome and transcriptome sequencing has revealed that many basal metazoans and some pre-metazoans also have homologs of the TLR-to-NF-κB pathway (Gilmore and Wolenski, 2012). However, the biological roles of TLR and NF-κB in these basal organisms are not well understood (Bosch et al., 2009).

In mammals, TLRs are single-pass transmembrane proteins with an N-terminal extracellular leucine-rich repeat (LRR) domain, a central transmembrane (TM) domain, and a C-terminal

Abbreviations: IKK, IkappaB kinase; LRR, leucine-rich repeat domain; Nv, *Nematostella vectensis*; NF-κB, nuclear factor kappa B; Of, *Orbicella faveolata*; TIR, Toll/interleukin-1 receptor; TLR, Toll-like Receptor; TM, transmembrane.

* Corresponding author. Biology Department, Boston University, 5 Cummington Mall, Boston, MA 02215, USA.
E-mail address: gilmore@bu.edu (T.D. Gilmore).

https://doi.org/10.1016/j.dci.2017.10.016
0145-305X/

intracellular Toll/interleukin-1 receptor (TIR) domain. Ligand recognition by the LRR domain promotes engagement of the intracellular TIR domain with other TIR domain-containing adapter proteins, which initiates downstream signaling cascades (Kawai and Akira, 2007). These adapter proteins include myeloid differentiation primary response protein 88 (MYD88), TIR domain-containing adapter protein (TIRAP/MAL), TIR domain-containing adapter inducing IFNβ (TRIF), and Trif-related adapter protein (TRAM) (Aderem and Ulevitch, 2000; Kawai and Akira, 2007). The number of TLRs varies widely among organisms, with ten TLRs in humans, 13 in mice, nine in fruit flies, and over 200 in sea urchins (Buckley and Rast, 2012; Valanne et al., 2011; Vasselon and Detmers, 2002). In more basal organisms, such as sponges and cnidarians (which include hydras, jellyfish, sea anemones, and corals), there are two types of TLR-like proteins. Most often, these basal TLR-like proteins contain only a TM domain and a TIR domain; however, some basal animals have genes encoding full-length TLRs with LRR, TM, and TIR domains, similar to mammalian TLRs. Within the phylum Cnidaria, there are animals having no complete TLRs (*Aiptasia pallida*, *Hydra vulgaris*), ones having one complete TLR (*Nematostella vectensis*), and ones having multiple complete TLR and TLR-like proteins (*Acropora digitifera*) (Miller et al., 2007; Poole and Weis, 2014; Shinzato et al., 2011).

In insects and mammals, the NF-κB superfamily comprises multiple related transcription factors that bind distinct DNA sequences known as κB sites (Hayden and Ghosh, 2004). All NF-κB proteins have a conserved N-terminal domain of approximately 300 amino acids called the Rel Homology Domain (RHD). The RHD has residues important for DNA binding, dimerization, and nuclear localization (Gilmore, 2006). The NF-κB superfamily can be divided into two subclasses: the NF-κB proteins (e.g., human p52/p100 and p50/p105, and *Drosophila* Relish) and the Rel proteins (e.g., human p65/RelA, c-Rel, and RelB, and *Drosophila* Dorsal and Dif) (Gilmore, 2006). Based on DNA binding-site preference and sequence similarity, the NF-κB RHDs are more related to each other than to the RHDs of Rel proteins (Finnerty and Gilmore, 2015; Siggers et al., 2011). Where characterized, basal organisms (e.g., cnidarians, sponges, pre-metazoans) have single NF-κB family proteins, which are phylogenetically most similar to the vertebrate and insect NF-κB subclass (Finnerty and Gilmore, 2015).

In addition to the RHD, members of the NF-κB subclass have a C-terminal inhibitory domain consisting primarily of a series of Ankyrin (ANK) repeats, which must be removed by proteolysis to activate the DNA-binding activity of the transcription factor (Hayden and Ghosh, 2004; Sun, 2011). For example, the vertebrate NF-κB proteins p100 and p105 are processed to p52 and p50, respectively, which then translocate from the cytoplasm to the nucleus. In the mammalian non-canonical NF-κB signaling pathway, IκB kinase (IKK)-mediated phosphorylation of p100 at three serine residues located C-terminal to the ANK repeats promotes its processing to p52 by the proteasome (Sun, 2011). On the other hand, the *Drosophila melanogaster* NF-κB protein Relish is activated by a discrete caspase-mediated proteolytic event that removes the C-terminal ANK repeat domain (Stöven et al., 2003; Valanne et al., 2011). Overall, it is not known how NF-κB proteins are regulated and activated in organisms basal to *Drosophila*.

The mountainous star coral *Orbicella faveolata* (*Of*), previously known as *Montastraea faveolata*, is an endangered reef-building coral found in the Caribbean Sea and the Gulf of Mexico. *O. faveolata* forms a symbiotic relationship with a dinoflagellate of the genus *Symbiodinium* (Davy et al., 2012; Steele et al., 2011). Like most reef-building corals, *O. faveolata* is susceptible to an environmentally induced loss of symbiosis, commonly referred to as "bleaching" because this process gives the coral tissue a white appearance (Brown, 1997; Gleason and Wellington, 1993; Hoegh-Guldberg et al., 2007; Hughes et al., 2017; Weis, 2008). Bleaching often causes coral death, but in some cases, corals can recover from a bleaching event and re-establish a symbiotic relationship with *Symbiodinium*. Nevertheless, recovered corals often show increased susceptibility to microbial diseases such as yellow band disease, black band disease, and plague (Kushmaro et al., 1996; Pinzón et al., 2015).

Recent reports of transcriptional changes in immune-related molecules in bleached and pathogen-infected corals have suggested that the cnidarian innate immune system plays a role in coral diseases (Anderson et al., 2016; Fuess et al., 2016, 2017; Pinzón et al., 2015; Zhou et al., 2017). To gain deeper insights into molecular processes important for coral immunity and health, we have had an ongoing interest in characterizing cnidarian homologs of mammalian immunoregulatory molecules and pathways (Wolenski et al., 2011, 2013). In this report, we have used phylogenetic, biochemical, and cell-based assays to characterize the structure, activity, and regulation of TLR and NF-κB proteins from *O. faveolata*. We also show that lipopolysaccharide (LPS) treatment of *O. faveolata* tissue can induce a gene expression profile consistent with induction of the NF-κB pathway. These results represent the first characterization of proteins in the conserved immunoregulatory TLR-to-NF-κB pathway of a critically endangered coral.

2. Materials and methods

2.1. Phylogenetic analyses

For comparative analysis of Toll-like receptors, the predicted TIR domains of *Orbicella faveolata* (Of) TLR, *Nematostella vectensis* (Nv) TLR, *Drosophila melanogaster* (Dm) Toll, and an *Amphimedon queenslandica* (Aq) TLR-like protein (Gauthier et al., 2010) were analyzed along with the ten human TLR proteins. The TIR domains of Of-TLR, Nv-TLR, and Aq-TLR were identified through MEME analysis (Bailey et al., 2006), and sequences were trimmed to contain only the TIR domains based on motif prediction and known human TIR domains (Supplemental Table 1). Human TLR and Dm-Toll amino acid sequences, along with their annotated TIR domains, were obtained from the UniProt database. Clustal Omega (Sievers et al., 2011) was then used to align the trimmed and culled TIR sequence dataset. The tree was rooted with the Aq-TLR, and phylogenetic comparison was performed using neighbor-joining analysis bootstrapped 1000 times using PAUP* (Swofford, 2001).

For phylogenetic analysis of the NF-κB and Rel proteins, the RHD sequences of *O. faveolata* (Of) NF-κB (from NCBI) *Aiptasia pallida* NF-κB (NCBI), *Actinia tenebrosa* NF-κB (NCBI), *N. vectensis* NF-κB (UniProt), *D. melanogaster* Relish, Dorsal, and Dif (UniProt), and *Homo sapiens* p100, p105, RelA, RelB, and c-Rel (UniProt) were obtained. The tree was rooted with an NF-κB-like protein from *Capsaspora owczarzaki* (NCBI). As described above, conserved motifs from MEME analysis (Bailey et al., 2006) were truncated based on motif predictions (see Supplemental Table 2), were aligned by Clustal Omega (Sievers et al., 2011), and were inputted into PAUP* (Swofford, 2001) for maximum likelihood analysis bootstrapped 1000 times.

2.2. Plasmid constructions, cell culture and transfections

Expression plasmids for HA-tagged human IKKβ, FLAG-Nv-NF-κB, FLAG-Hu-IKKβ, and the empty pcDNA-FLAG vector have been described previously (Starczynowski et al., 2007; Wolenski et al., 2011). cDNAs encoding human cell codon-optimized versions of Of-NF-κB, Of-IKK, and Of-TLR were synthesized (GenScript) (Supplemental Figs. 1, 2, and 3, respectively). These cDNAs and PCR-generated Of-NF-κB truncation mutants (Of-RHD and Of-Cterm)

were subcloned into pcDNA-FLAG or the yeast GAL4-fusion vector pGBT9. Details about primers and plasmid constructions are included in Supplemental Material (Supplemental Tables 3 and 4).

DF-1 chicken fibroblasts and human HEK 293 or 293T cells were grown in Dulbecco's modified Eagle's Medium (Invitrogen) supplemented with 10% fetal bovine serum (Biologos), 50 units/ml penicillin, and 50 μg/ml streptomycin as described previously (Wolenski et al., 2011). Transfection of cells with expression plasmids was performed using polyethylenimine (PEI) (Polysciences, Inc.) essentially as described previously (Sullivan et al., 2009; Wolenski et al., 2011). Briefly, on the day of transfection, cells were incubated with plasmid DNA and PEI at a DNA:PEI ratio of 1:6. Media was changed 24 h post-transfection, and whole-cell lysates were prepared 24 h later in AT Lysis Buffer (20 mM HEPES, pH 7.9, 150 mM NaCl, 1 mM EDTA, 1 mM EGTA, 20% wt/vol glycerol, 1% [wt/vol] Triton X-100, 20 mM NaF, 1 mM $Na_4P_2O_7 \cdot 10H_2O$, 1 mM dithiothreitol, 1 mM phenylmethylsulfonyl fluoride, 1 μg/ml leupeptin, 1 μg/ml pepstatin A, 10 μg/ml aprotinin). If cells were used for immunofluorescence, they were passaged onto glass coverslips on the day prior to fixation.

2.3. Glutathione-S-transferase (GST) pull-down assays

GST and GST-TIR domain fusion proteins were expressed in BL21 and BL21 pLyse bacterial cells, respectively, and were purified from extracts using glutathione beads as described previously (Garbati et al., 2010). To assess the amounts and sizes of the purified GST proteins 1% of GST and 10% of the GST samples were electrophoresed on a 10% SDS-polyacrylamide gel, which was then stained with Coomassie blue (Bio-Rad). The remaining portions of the GST proteins on beads were incubated with extracts from 293 cells expressing FLAG-MYD88. The beads were then washed four times with cold PBS, and were boiled in 2× SDS sample buffer to release proteins from the beads. Proteins were electrophoresed on a 7.5% SDS-polyacrylamide gel, and the gel was subjected to anti-FLAG Western blotting as described elsewhere (Wolenski et al., 2011) and below.

2.4. Western blotting, electrophoretic mobility shift assays (EMSAs), reporter gene assays, and indirect immunofluorescence

Western blotting for FLAG- and HA-tagged proteins was performed essentially as described previously (Wolenski et al., 2011), using a rabbit anti-FLAG (1:1000, Cell Signaling Technology) or anti-HA (1:500, Cell Signaling Technology) antisera. Briefly, samples were subjected to SDS-PAGE, proteins were transferred to nitrocellulose, incubated with primary antibody, and then with anti-rabbit horseradish peroxidase-linked secondary antibody (1:5000, Cell Signaling Technology). Immunoreactive proteins were detected with SuperSignal West Dura Extended Duration Substrate (Pierce). EMSAs were performed using a ^{32}P-labeled κB-site probe (GGGAATTCCC, see Supplemental Table 4) and 293 whole-cell extracts, as described previously (Wolenski et al., 2011). Yeast GAL4-site *LacZ* and 293 cell κB-site luciferase reporter gene assays were performed as described previously (Wolenski et al., 2011). Transfection and indirect immunofluorescence of DF-1 cells were performed essentially as described previously, and fixed cells were probed with rabbit anti-FLAG primary antiserum (1:50, Cell Signaling Technology) (Wolenski et al., 2011).

2.5. In vitro kinase assays

In vitro kinase assays were performed as described previously (Wolenski et al., 2011). Briefly, human 293T cells were transfected with pcDNA-FLAG-IKKβ and pcDNA-FLAG-Of-IKK constructs, lysed two days later, and the kinases were immunoprecipitated with anti-FLAG beads (Sigma). These immunoprecipitates were then incubated with approximately 4 μg of GST alone, GST-Of-NF-κB or GST-Of-NF-κB-3X-Ala C-terminal peptides and 5 μCi [γ-^{32}P]ATP (Perkin Elmer) in kinase reaction buffer (25 mM Tris-HCl, pH 7.5, 20 mM β-glycerophosphate, 10 mM NaF, 10 mM $MgCl_2$, 2 mM DTT, 500 μM Na_3VO_4, 50 μM ATP) for 30 min at 30 °C. Samples were then boiled in 2× SDS sample buffer and electrophoresed on a 10% SDS-polyacrylamide gel. The ^{32}P-labeled GST-Of-NF-κB peptides were detected by phosphorimaging. As a control for protein input, 4 μg of GST alone, GST-Of-NF-κB or GST-Of-NF-κB-3X-Ala was electrophoresed on a 10% SDS-polyacrylamide gel, and proteins were detected by staining with Coomassie blue (Bio-Rad).

2.6. RNA-seq and Ingenuity Pathway Analysis

The collection and maintenance of *O. faveolata* fragments have been described previously (Fuess et al., 2017). Collected *O. faveolata* were exposed to lipopolysaccharide (LPS) from *Escherichia coli* 0127:B8 (Sigma) at a final concentration of 10 μg/ml for 30 min, and samples were then aerated with seawater for 4 h before being removed and frozen in liquid nitrogen. Samples were lysed in a 50 mM Tris-base, pH 7.8, with 0.05 mM dithiothreitol, and then RNA was extracted, made into cDNA, and sequenced. Ingenuity Pathway Analysis was performed as described elsewhere (Fuess et al., 2017).

3. Results

3.1. Conservation of Toll-like receptor (TLR) pathway in Orbicella faveolata

To determine whether proteins in the vertebrate TLR-to-NF-κB innate immune pathway (Silverman and Maniatis, 2001) are present in the coral *O. faveolata*, we scanned transcriptomic data (Pinzón et al., 2015). Homologous transcripts of many of the receptor and downstream signaling components of the mammalian TLR pathway were present in *O. faveolata* (Fig. 1). Nevertheless, in many cases, there were reduced numbers of signaling components in each family (Supplemental Table 5). For example, there are five NF-κB/Rel proteins in humans, but there was a single NF-κB-like protein in *O. faveolata*. Similarly, there are ten complete TLRs in humans, but in *O. faveolata* there was only a single predicted full-length TLR and four TLR-like proteins containing only TM and TIR domains.

3.2. A predicted TLR-to-NF-κB pathway in Orbicella faveolata

From transcriptomic analysis, the single full-length Of-TLR is predicted to contain *bona fide* LRR, TM, and TIR domains. By phylogenetic analysis using the neighbor-joining method, the TIR domain of Of-TLR was most closely related to the TIR domains of the single characterized *N. vectensis* (Nv) TLR (Brennan et al., 2017) and to the *D. melanogaster* Toll protein. Among the human TLRs, Of-TLR appeared to be most similar to the TIR domain of human TLR4 (Fig. 2A).

Since the TIR domain of human TLR4 interacts with the intracellular adapter protein MYD88 as an early step in signaling to NF-κB (O'Neill et al., 2003), we sought to determine whether the TIR domain of Of-TLR (Of-TIR) could also interact with human MYD88. We incubated bacterially expressed GST-Of-TIR with 293 cell extracts overexpressing FLAG-MYD88, and performed a pull-down assay (Fig. 2B). As shown in Fig. 2C, MYD88 was detected by Western blotting in pull-down fractions containing GST-Of-TIR, but MYD88 was not seen with GST alone. As a positive control, we

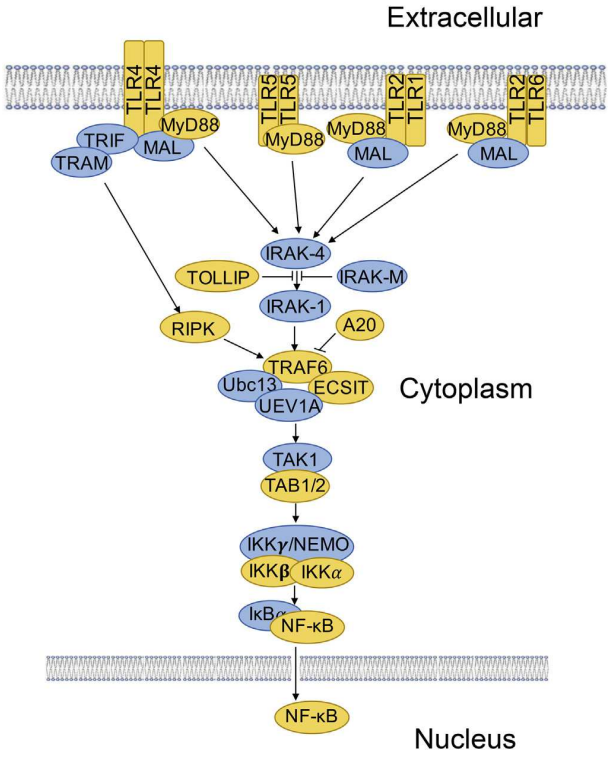

Fig. 1. Homologs of proteins in the mammalian Toll-Like Receptor-to-NF-κB pathway are present in *Orbicella faveolata*. Transcriptomic data of *O. faveolata* from Pinzón et al. (2015) were mined and found to contain RNAs encoding many receptor and downstream signaling components of the mammalian TLR-to-NF-κB pathway. TLR signaling components that are only found in humans are in blue, and those human pathway components with homologs in *O. faveolata* are in yellow. TLR1, 2, 5, and 6 homologs in *O. faveolata* are TIR domain-only proteins. (For interpretation of the references to colour in this figure legend, the reader is referred to the web version of this article.)

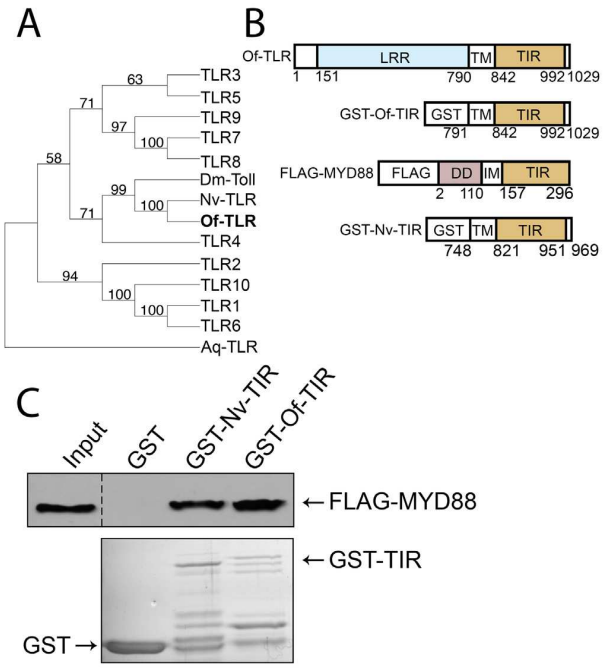

Fig. 2. Similarity of Of-TLR to human TLR4. (A) Phylogenetic analysis of the TIR domains of the indicated TLR proteins was performed using neighbor-joining tree analysis bootstrapped 1000 times. The phylogeny was rooted with the TIR domain of a TLR-like protein of the sponge *A. queenslandica*. Branches indicate bootstrap support values. Of, *O. faveolata*; Nv, *N. vectensis*; Aq, *A. queenslandica*. TLR1-10 are the human TLR proteins. (B) Schematic structures of Of-TLR (1029 amino acids) and the GST-TIR and FLAG-MYD88 constructs used in pull-down assays. Highlighted are conserved structural components shared with other TLR and adapter proteins: LRR, leucine-rich region; TM, transmembrane domain; TIR, Toll/interleukin-1 receptor; DD, death domain, IM, intermediary domain. (C) Pull-down assays with GST and GST-TIR, and FLAG-tagged MYD88. The top panel shows an anti-FLAG Western blot of pull-downs using GST, GST-Nv-TIR or GST-Of-TIR. The input lane contains 0.7% of the FLAG-MYD88 293 cell lysate used in the pull-downs. Expression of bacterially expressed GST proteins was confirmed by SDS-PAGE followed by Coomassie blue staining (bottom). Dashed line represents the merge of Western blot lanes from a single gel. (Note: so that the amounts of GST proteins analyzed in the pull-downs were more similar, one-half of the sample from the GST alone pull-down was loaded on the gel used in the Western blot.).

showed that MYD88 also interacted with GST-Nv-TIR, which we have recently shown can interact with human MYD88 (Brennan et al., 2017). Thus, the phylogenetic similarity of Of-TLR and human TLR4 proteins was reinforced functionally by Of-TLR's ability to interact with the human TLR4 adapter protein MYD88.

Having established that Of-TLR had similarities to human TLR4, we sought to determine whether *O. faveolata* tissue would elicit a response to gram-negative lipopolysaccharide (LPS), an activator of the mammalian TLR4-to-NF-κB pathway. Therefore, we treated *O. faveolata* tissue for 30 min with LPS, and followed that treatment with a 4-h washout period with seawater. RNA was then extracted from treated tissues and subjected to RNA-seq analysis. Ingenuity Pathway Analysis (IPA) of the RNA-seq data identified 39 pathways in *O. faveolata* that were significantly activated (as compared to control tissue), and 13 of these pathways had numerical z-scores. Of these 13 pathways, NF-κB signaling was the most significantly activated pathway (IPA: z-score = 1.8, $p = 0.03$) (Fuess et al., 2017). A total of 16 genes in the NF-κB signaling pathway were expressed in our samples, resulting in a 9.3 E^{-02} pathway ratio (Table 1). Among the NF-κB pathway components activated by LPS treatment were the following: TLR1-and 2-like proteins; members of the tumor necrosis factor receptor associated factor family (TRAF2, 3, 5), which are proteins involved with regulation of the pathway; kinases including RIPK1, MAP3K3, and PIK3R4; and the adapter protein MYD88. Nearly all genes in the NF-κB signaling pathway were up- or down-regulated in a manner that was consistent with activation of the pathway as it known in mammalian systems (Table 1).

3.3. The structure and phylogenetic analysis of the O. faveolata NF-κB protein indicates that it is more similar to mammalian NF-κB proteins than to Rel proteins

Because IPA predicted that LPS could activate the NF-κB pathway in *O. faveolata*, we sought to characterize NF-κB-like proteins in *O. faveolata*. By scanning an *O. faveolata* transcriptomic database (Pinzón et al., 2015), we identified transcripts encoding a single NF-κB-like protein, but no Rel-like protein. The amino acid sequence of the Of-NF-κB protein (Supplemental Fig. 1) indicated that it had an overall domain structure that was most similar to mammalian NF-κB proteins, i.e., with an N-terminal RHD, followed by a glycine-rich region, and then a series of ANK repeats (Fig. 3A). A maximum-likelihood analysis of Of-NF-κB also indicated that it was most similar to other invertebrate NF-κB proteins, most notably those from sea anemones (*N. vectensis*, *Aiptasia* sp, and *A. tenebrosa*) (Fig. 3B). Moreover, Of-NF-κB clustered with NF-κB proteins from *D. melanogaster* (Relish) and humans (p100 and

Table 1
NF-κB pathway genes differentially expressed following LPS treatment on *O. faveolata*.

Gene	Number of Contigs	Average Log_2 Fold Change	Standard Error	Function	Activation Status
TRAF2	1	2.7	N/A	Enzyme	Consistent
RIPK1	1	2.6	N/A	Kinase	Consistent
FGFRL1	1	1.8	N/A	Transmembrane receptor	Consistent
FGFR4	1	1.4	N/A	Kinase	Consistent
TRAF3	8	0.8	0.43	Enzyme	Consistent
TLR2-like	4	0.6	1.00	Transmembrane receptor	Not predicted
TRAF5	9	0.5	0.30	Transporter	Consistent
FGFR1	3	0.4	0.01	Kinase	Consistent
MAP3K3	3	0.4	0.51	Kinase	Consistent
BMP2	2	0.3	0.87	Growth factor	Consistent
MALT1	3	0.2	0.53	Peptidase	Consistent
IGF2R	1	−0.3	N/A	Transmembrane receptor	Not predicted
TLR1-like	2	−0.6	0.97	Transmembrane receptor	Not predicted
TDP2	2	−0.7	0.60	Transcription regulator	Inconsistent
MYD88	2	−0.7	0.24	Other	Inconsistent
PIK3R4	2	−1.4	1.08	Kinase	Consistent

O. faveolata tissue was exposed to *E. coli* LPS for 30 min and then returned to seawater for 4 h. RNA-seq was performed to identify transcripts whose expression was affected by this treatment, and Ingenuity Pathway Analysis was then used to identify pathways whose gene expression patterns were significantly changed by LPS treatment. The "NF-κB pathway" was found to be the most significantly activated pathway overall. Listed are 16 *O. faveolata* genes with homologs in the NF-κB pathway whose expression was affected by LPS treatment. Average Log_2-Fold Change is indicated as well as associated error, encoded protein function from IPA analysis (Function), and consistency with pathway activation (Activation Status). The complete RNA-seq dataset for differently expressed genes can be found in Fuess et al. (2017).

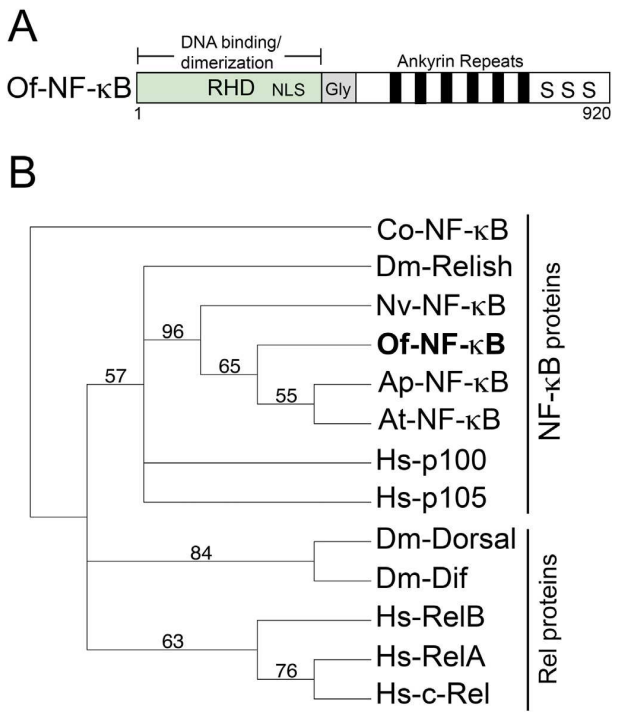

Fig. 3. Of-NF-κB is most similar to other NF-κB proteins and not to Rel proteins. (A) Schematic linear structure of the Of-NF-κB protein (920 amino acids). Highlighted are functional domains shared with mammalian NF-κB proteins: RHD, Rel Homology Domain; NLS, Nuclear Localization Sequence; Gly, glycine-rich region; S, serine; vertical black bars, Ankyrin repeats. (B) Phylogenetic analysis of the RHDs of the indicated NF-κB and Rel proteins using maximum-likelihood analysis bootstrapped 1000 times. The phylogeny was rooted with the NF-κB protein of the single-celled eukaryote *Capsaspora owczarzaki*. Branches indicate bootstrap support values. Co, *Capsaspora owczarzaki*; Of, *Orbicella faveolata*; Nv, *Nematostella vectensis*; Ap, *Aiptasia pallida;* Hs, *Homo sapiens.*

p105), and was distinct from the Rel proteins. This result is similar to the clustering of Nv-NF-κB with NF-κB proteins, but distinct from Rel proteins, as reported by Sullivan et al. (2007).

3.4. C-terminal truncation of the O. faveolata NF-κB protein is required for nuclear localization, DNA binding, and transactivation

The mammalian NF-κB proteins p100 and p105 require removal of their C-terminal ANK repeat domain in order to become active transcription factors. Due to the structural similarity of Of-NF-κB to human NF-κB p100 and p105, we sought to determine whether C-terminal truncation of Of-NF-κB would unveil active transcription factor properties. Therefore, we created expression vectors for FLAG-tagged codon-optimized versions of full-length Of-NF-κB, an N-terminal form (Of-RHD), and a protein containing only the C-terminal glycine-rich and ANK repeat domain (Of-Cterm) (Fig. 4A). As a control, we used an expression vector for the 440 amino acid *N. vectensis* NF-κB protein (Nv-NF-κB), which we have characterized previously as an active NF-κB protein (Wolenski et al., 2011). Each of the Of-NF-κB constructs directed the expression of an appropriately sized protein when transfected into HEK 293 cells (Fig. 4B).

To determine the subcellular localization of the Of-NF-κB proteins, we transfected the plasmids into chicken fibroblasts and later performed anti-FLAG indirect immunofluorescence. We found that full-length Of-NF-κB and Of-Cterm were present in the cytoplasm of transfected chicken fibroblasts, whereas Of-RHD and the control Nv-NF-κB protein were both located in the nucleus of these cells (Fig. 4C).

We next analyzed the DNA-binding and transactivation properties of the full-length and truncated Of-NF-κB proteins. To measure DNA-binding activity, 293 cells were transfected with the Of-NF-κB expression plasmids, and extracts were analyzed for DNA-binding activity by an electrophoretic mobility shift assay (EMSA) using a κB-site probe that we have previously shown can be avidly bound by Nv-NF-κB (Wolenski et al., 2011). Lysates from cells transfected with expression plasmids for Of-RHD and the positive control Nv-NF-κB both contained proteins that strongly bound to the κB-site probe (Fig. 4D). In contrast, extracts from cells transfected with the empty vector control, Of-NF-κB or Of-Cterm showed only low or background κB-site DNA-binding activity (Fig. 4D). In addition, Of-RHD and Nv-NF-κB both activated transcription of an NF-κB-responsive luciferase reporter plasmid when overexpressed in 293 cells as compared to empty vector control-transfected cells (Fig. 4E). As expected, full-length Of-NF-κB and

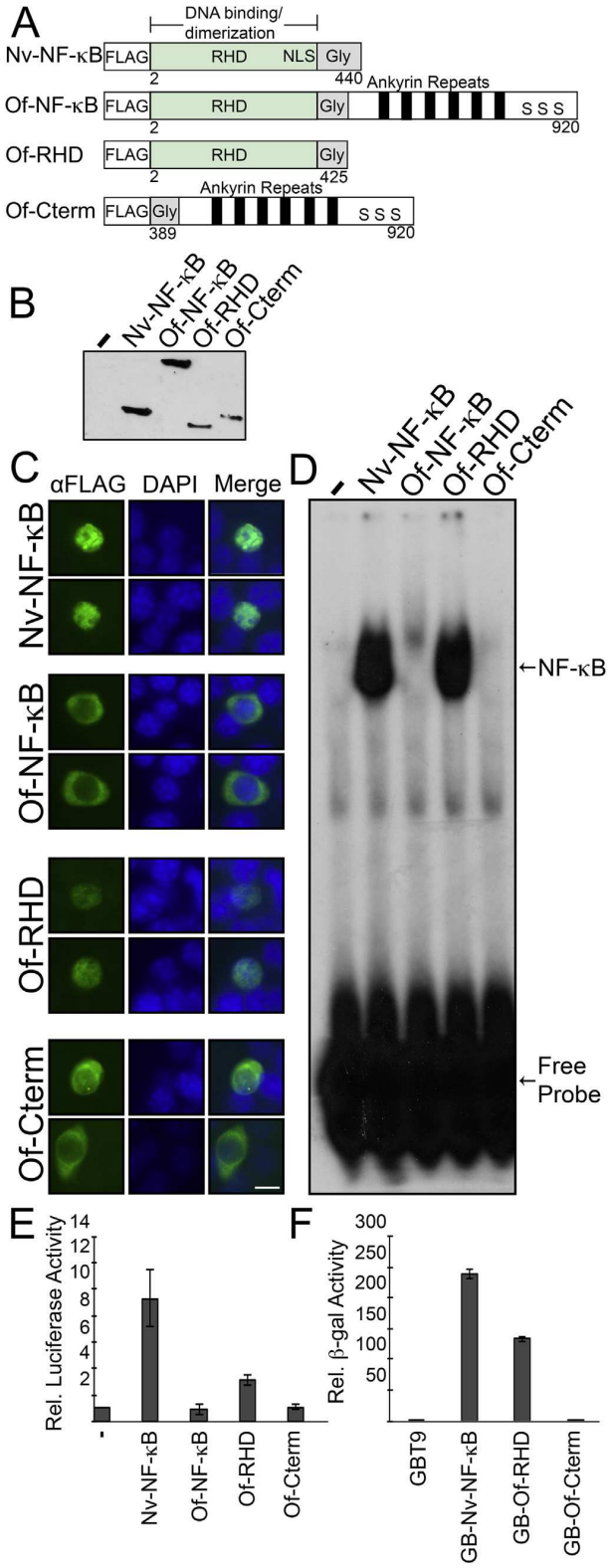

Fig. 4. Characterization of the activity of the *O. faveolata* NF-κB protein in cell-based assays. (A) FLAG-tagged expression vectors used in these experiments. Shown from top to bottom are generalized structures of the naturally shortened Nv-NF-κB, full-length Of-NF-κB, a C-terminal truncation mutant of Of-NF-κB (Of-RHD), and an N-terminal deletion mutant of Of-NF-κB possessing only the glycine-rich region and the Ankyrin repeats (Of-Cterm). (B) An anti-FLAG Western blot of lysates from 293 cells transfected with the indicated plasmid expression vectors. (C) Chicken DF-1 fibroblasts were transfected with pcDNA-FLAG vectors containing the indicated proteins, and three days later cells were analyzed by anti-FLAG (αFLAG) indirect immunofluorescence (left, green) and DAPI staining (middle, blue). Merged images are shown in the right panels. Scale bar = 10 μm. (D) Top: A κB-site EMSA using lysates from 293 cells expressing the indicated FLAG-tagged proteins, as shown in (B). Arrows indicate the free probe and the shifted NF-κB-DNA complex. (E) A κB-site luciferase reporter gene assay was performed with the indicated proteins in 293 cells. Luciferase activity is relative (Rel.) to that seen with the empty vector control (1.0), and values are the averages of three assays performed with triplicate samples with standard error. (F) A GAL4-site *LacZ* reporter gene assay was performed in yeast Y190 cells. β-galacotisidase (β-gal) reporter gene activity is relative (Rel.) to the GAL4 (aa 1-147) control (1.0), and values are the averages of seven assays performed with duplicate samples with standard error. (For interpretation of the references to colour in this figure legend, the reader is referred to the web version of this article.)

Of-Cterm did not activate the reporter above vector control levels (Fig. 4E). Taken together, these results showed that removal of C-terminal ANK repeat domain sequences of Of-NF-κB enabled the protein to enter the nucleus, bind to DNA, and activate transcription in vertebrate cells.

To further demonstrate that Of-NF-κB was a functional transcriptional activator, we assessed its ability to activate transcription in yeast, which do not have endogenous NF-κB proteins. To accomplish this, we fused the Of-RHD to the GAL4 DNA-binding domain (GAL4-Of-RHD) and expressed this protein in yeast cells, which contain an integrated GAL4-site *LacZ* reporter locus. In these cells, GAL4-Of-RHD activated transcription of the GAL4-site reporter substantially (~135-fold) above control (GAL4 alone) levels. However, the GAL4-Cterm fusion protein did not activate transcription of the reporter in yeast (Fig. 4F). As we have shown previously (Alshanbayeva et al., 2015; Wolenski et al., 2011), a GAL4-Nv-NF-κB fusion protein strongly (~240-fold) activated transcription in yeast as compared to the GAL4 alone control. Therefore, the ability of the Of-RHD sequences to activate transcription appeared to be conserved from yeast to human cells, and appeared to be an intrinsic property of sequences within the N-terminal half of the protein.

3.5. C-terminal truncation of of-NF-κB can be induced by an IKK-dependent mechanism in human cells

Upon activation, the human NF-κB p100 protein is converted to its active p52 form by proteasomal processing of C-terminal sequences up to the glycine-rich region (Sun, 2011). This processing is initiated by IKK-dependent phosphorylation of a cluster of three serine residues located C-terminal to the ANK repeats of p100 (Sun, 2011). The Of-NF-κB protein contains three serine residues with similar spacing and flanking sequences to the IKK target serines in human p100 and in an NF-κB protein from the sea anemone *A. pallida* (Fig. 5A). In an *in vitro* kinase assay (Fig. 5B), a constitutively active form of human IKKβ and the predicted Of-IKK protein could each phosphorylate a bacterially expressed GST-fusion peptide containing the C-terminal serine residues of Of-NF-κB (amino acids 843-874); however, neither IKK phosphorylated the analogous GST-fusion protein containing alanine substitutions for the three serine residues or GST alone (Fig. 5B).

To determine whether IKK-dependent phosphorylation could induce processing of Of-NF-κB, we transfected human 293T cells with expression vectors for FLAG-Of-NF-κB and either FLAG-Of-IKK or HA-Hu-IKKβ, which we have recently shown can induce processing of the sea anemone *A. pallida* NF-κB protein in similar experiments (Mansfield et al., 2017). As shown in Fig. 5C, co-transfection of 293T cells with FLAG-Of-NF-κB and either FLAG-Of-IKK or HA-Hu-IKKβ resulted in the appearance of an Of-NF-κB

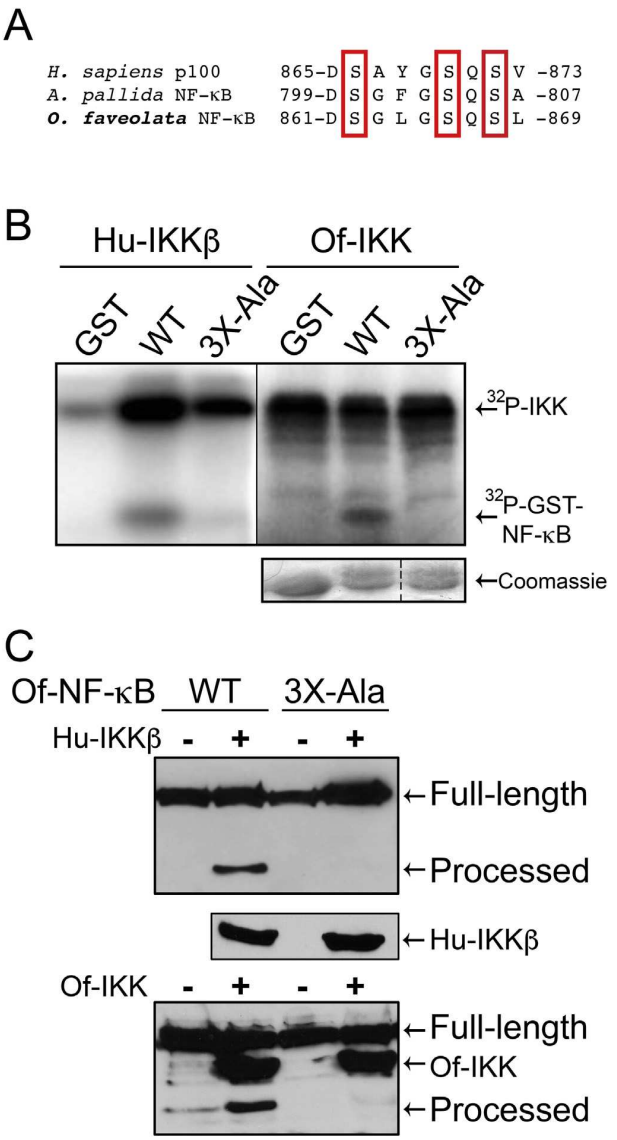

Fig. 5. IKK can phosphorylate conserved serines in Of-NF-κB *in vitro* and induce processing of Of-NF-κB in human cells. (A) An alignment of relevant regions of NF-κB from human p100, the sea anemone *A. pallida*, and *O. faveolata*. Conserved serine residues are boxed in red. (B) *In vitro* kinase assay (top) using a constitutively active FLAG-Hu-IKKβ protein and FLAG-Of-IKK with bacterially expressed substrates of GST alone or GST fusion proteins containing the wild-type (WT) serine residues of Of-NF-κB (amino acids 843-874), or the same C-terminal residues with conserved serines mutated to alanines (3X-Ala). The GST proteins were electrophoresed on an SDS-polyacrylamide gel and stained with Coomassie blue (bottom). Dashed lines indicate the respective Coomassie blue stain for each protein. (C) A Western blot of lysates from 293T cells co-transfected with Of-NF-κB wild-type (WT) or 3X-Ala and with HA-Hu-IKKβ (top two panels) or FLAG-Of-IKK (bottom panel). Full-length and processed forms of Of-NF-κB are indicated. Shown also are the HA-Hu-IKKβ (middle panel) and FLAG-Of-IKK proteins (bottom panel) from the same lysates. (For interpretation of the references to colour in this figure legend, the reader is referred to the web version of this article.)

band of approximately 50 kDa. No such smaller band was seen when the Of-NF-κB-3X-Ala mutant was co-transfected with FLAG-Of-IKK or HA-Hu-IKKβ. Together, these results indicate that Of-NF-κB can undergo IKK-induced processing in human cells, and that this processing requires conserved sites of IKK-directed phosphorylation.

4. Discussion

The data presented in this paper suggest that there are highly conserved elements of a TLR-to-NF-κB innate immune pathway in the endangered coral *O. faveolata*. That is, we show that the intracellular TIR domain of the single Of-TLR protein is most similar by phylogenetic analysis to human TLR4, and that the TIR domain of Of-TLR can directly interact with human MYD88 (Fig. 2), which is an essential adapter protein for human TLR4-based signaling to NF-κB. Moreover, the single Of-NF-κB protein has sequence similarity, an overall structural organization, and transactivation properties that are more like human NF-κB proteins than human Rel proteins (Figs. 3 and 4). Furthermore, the Of-NF-κB protein can be processed in response to overexpression of human and *O. faveolata* IKK proteins in a manner consistent with non-canonical pathway processing of NF-κB p100 in human cells (Fig. 5). Finally, we show that a mammalian ligand of TLR4-to-NF-κB activation, namely gram-negative bacterial LPS, activates a gene expression profile in isolated *O. faveolata* tissue that is consistent with overall activation of NF-κB pathway genes (Table 1).

To date, a handful of studies have identified TLR-to-NF-κB pathway components in environmentally stressed cnidarians. Anderson et al. (2016) and Pinzón et al. (2015) identified transcripts encoding NF-κB signaling components in their transcriptomes from bleached *O. faveolata*. In the coral *Acropora palmata*, transcripts for a putative tumor necrosis factor receptor-associated factor 3 (TRAF3) homolog and NF-κB were shown to be upregulated when coral were exposed to increased water temperature (DeSalvo et al., 2010). The upregulation of NF-κB pathway components at the transcriptional level has also recently been described in the sea anemone *A. pallida* following treatment with heat or chemicals that induce bleaching (Mansfield et al., 2017). However, the precise mechanisms by which these conserved signal transduction pathways elicit their responses, the gene targets regulated by NF-κB in these organisms, and their biological roles in these cnidarians remain largely unknown.

Treatment of *O. faveolata* tissue with LPS results in significant differential expression of genes in a manner indicating activation of the NF-κB pathway. These results are consistent with other studies that have reported upregulation of NF-κB pathway transcripts as a response to pathogen-induced stress in cnidarians. For example, Franzenburg et al. (2012) demonstrated that microbial infection of *Hydra* elicits a TLR-like pathway response and bacterial flagellin can activate TLR-to-NF-κB signaling when the *Hydra* TLRs are expressed in mammalian cells (Bosch et al., 2009). Similarly, Brennan et al. (2017) have shown that a coral bacterial pathogen can activate the *N. vectensis* TLR. However, our results are the first to show that NF-κB pathway components in an endangered coral are upregulated in response to treatment with a known mammalian inducer of NF-κB, i.e., LPS (Table 1). Whether this activation of NF-κB components by LPS occurs through the Of-TLR that we characterize here is not known.

Although our results suggest a link between LPS treatment and activation of NF-κB in *O. faveolata*, it is important to note the differences between our findings and the LPS-induced rapid activation of NF-κB that is usually studied in mammalian systems. That is, our results show that the levels of mRNAs encoding several NF-κB pathway components are upregulated approximately 4 h after treatment of *O. faveolata* tissue with LPS. In contrast, LPS-induced activation of NF-κB in mammalian systems is usually studied as the rapid nuclear localization of a latent cytoplasmic NF-κB complex approximately 10–30 min following treatment with LPS. Thus, we have not directly shown that LPS treatment activates the NF-κB protein in a conventional sense.

Our results suggest that the TLR-to-NF-κB pathway in

O. faveolata has characteristics of both non-canonical and canonical NF-κB signaling in mammals. On the one hand, the Of-NF-κB pathway is like the mammalian non-canonical pathway in that 1) the overall organization of Of-NF-κB is similar to the mammalian NF-κB protein p100, 2) C-terminal truncation leads to nuclear localization, enhanced DNA binding, and enhanced transactivation in vertebrate cells, 3) IKKs can induce partial processing of over-expressed Of-NF-κB in human cells, 4) sites of IKK-dependent serine phosphorylation in p100 are conserved in Of-NF-κB, and 5) these serine residues are required for processing of Of-NF-κB in human cells. On the other hand, human IKKβ, which is normally associated with canonical NF-κB signaling in mammalian cells, is as active as, if not even more active than, Of-IKK towards Of-NF-κB in our *in vitro* phosphorylation and human cell induction experiments. Moreover, TLR4 generally activates the canonical NF-κB pathway in mammalian cells. Furthermore, although the TIR domain of the Of-TLR has properties of human TLR4, the extracellular LRR domain of Of-TLR is more similar to the *Drosophila* Toll protein (a multiple cysteine cluster TLR) than to TLR4 (a single cysteine cluster TLR), similar to what is seen with Nv-TLR (Brennan et al., 2017). Finally, the clustering of the TIR domain of Of-TLR with human TLR4 is not seen with other methods of phylogenetic analysis (e.g., maximum-likelihood and maximum parsimony [data not shown]). Thus, the evolutionary processes by which cnidarian TLR and TLR-like proteins, as well as a single cnidarian IKK, diversified into the multiple member higher metazoan TLR and IKK families vis-à-vis canonical vs. non-canonical signaling to NF-κB are not obvious.

Coral bleaching and coral pathogen disease will be persistent problems as ocean temperatures continue to rise as a result of climate change. Defining the biological processes and molecular pathways that are altered in bleached and diseased corals will likely be critical for determining how these organisms respond and survive. Moreover, given the broad impact that the understanding of immune pathways has had on human disease diagnosis and therapy, our data will no doubt contribute to the understanding of diseases in environmentally sensitive organisms as well. Thus, our characterization of key conserved immune regulatory molecules, namely TLR and NF-κB, in an endangered coral is an important contribution to molecular ecology and comparative immunology.

Acknowledgments

This research was supported by National Science Foundation grants IOS-1354935 (T.D.G.), IOS-1017458 (L.M.), and OCE-1712134 (L.M.). L.M.W. and L.E.F. were supported by NSF Graduate Research Fellowships, and K.M.M. was supported by a Warren-McLeod Graduate Fellowship in Marine Biology. E.S.R. was supported by NSF-REU BIO-1659605 (T.D.G.) and J.W. was supported by the Boston University GROW program. Designated authors performed research as part of the undergraduate project laboratory course BB522 (Spring 2016), and were supported by funds from the BU Biology Department. Special thanks to Adam Clemens for assistance in aligning codon-optimized protein sequences, and to Joshua Aguirre, Milad Babaei, Chris DiRusso, Jessica Keenan, Yuekun Liu, and Nima Mohaghegh for helpful discussions.

Appendix A. Supplementary data

Supplementary data related to this article can be found at https://doi.org/10.1016/j.dci.2017.10.016.

References

Aderem, A., Ulevitch, R.J., 2000. Toll-like receptors in the induction of the innate immune response. Nat. Lond 406, 782–787. https://doi.org/10.1038/35021228.

Akira, S., Uematsu, S., Takeuchi, O., 2006. Pathogen recognition and innate immunity. Cell 124, 783–801. https://doi.org/10.1016/j.cell.2006.02.015.

Alshanbayeva, A., Thomas, A., Tremblay, M., Abbas, M., Abdurrob, F., Almojel, T., Aparicio, A., Asarpota, D., Ayers, A., Aziz, A., Bishop, J., Christie, T., Chua, M.J., Melissa, Chung, O., Dhar, N., Diedrich, A., Fortin, C., He, Q., Heerboth, S., Hok, R., Khedkar, A., Kitchloo, S., Lawlor, C., Leonard, B., Linderman, S., Maloyan, M., Miller, L., Pak, C., Pandita, A., Park, I., Patel, N., Ramachandran, J., Reynoso, M., Samaha, Y., Thole, G., Turnbill, J., Xia, L., Zhu, J., Navarro, C., Gilmore, T.D., 2015. N- and C-terminal non-conserved residues contribute to transactivation by a sea anemone (Nematostella vectensis) NF-κB transcription factor. BIOS 86, 165–175. https://doi.org/10.1893/0005-3155-86.4.165.

Anderson, D.A., Walz, M.E., Weil, E., Tonellato, P., Smith, M.C., 2016. RNA-Seq of the Caribbean reef-building coral *Orbicella faveolata* (Scleractinia-Merulinidae) under bleaching and disease stress expands models of coral innate immunity. PeerJ 4, e1616. https://doi.org/10.7717/peerj.1616.

Bailey, T.L., Williams, N., Misleh, C., Li, W.W., 2006. MEME: discovering and analyzing DNA and protein sequence motifs. Nucleic Acids Res. 34, W369–W373. https://doi.org/10.1093/nar/gkl198.

Bosch, T.C.G., Augustin, R., Anton-Erxleben, F., Fraune, S., Hemmrich, G., Zill, H., Rosenstiel, P., Jacobs, G., Schreiber, S., Leippe, M., Stanisak, M., Grötzinger, J., Jung, S., Podschun, R., Bartels, J., Harder, J., Schröder, J.-M., 2009. Uncovering the evolutionary history of innate immunity: the simple metazoan *Hydra* uses epithelial cells for host defence. Dev. Comp. Immunol. 33, 559–569. https://doi.org/10.1016/j.dci.2008.10.004.

Brennan, J.J., Messerschmidt, J.L., Williams, L.M., Matthews, B.J., Reynoso, M., Gilmore, T.D., 2017. A sea anemone model has a single Toll-like receptor that can function in pathogen detection, NF-κB signal transduction, and development. Proc. Natl. Acad. Sci. U. S. A. (in press).

Brown, B.E., 1997. Coral bleaching: causes and consequences. Coral Reefs 16, S129–S138. https://doi.org/10.1007/s003380050249.

Buckley, K.M., Rast, J.P., 2012. Dynamic evolution of Toll-like receptor multigene families in echinoderms. Front. Immunol. 3, 136. https://doi.org/10.3389/fimmu.2012.00136.

Davy, S.K., Allemand, D., Weis, V.M., 2012. Cell biology of cnidarian-dinoflagellate symbiosis. Microbiol. Mol. Biol. Rev. 76, 229–261. https://doi.org/10.1128/MMBR.05014-11.

DeSalvo, M.K., Sunagawa, S., Voolstra, C.R., Medina, M., 2010. Transcriptomic responses to heat stress and bleaching in the elkhorn coral *Acropora palmata*. Mar. Ecol. Prog. Ser. 402, 97–113. https://doi.org/10.3354/meps08372.

Finnerty, J.R., Gilmore, T.D., 2015. Methods for analyzing the evolutionary relationship of NF-κB proteins using free, web-driven bioinformatics and phylogenetic tools. Methods Mol. Biol. 1280, 631–646. https://doi.org/10.1007/978-1-4939-2422-6_37.

Franzenburg, S., Fraune, S., Künzel, S., Baines, J.F., Domazet-Lošo, T., Bosch, T.C., 2012. MyD88-deficient Hydra reveal an ancient function of TLR signaling in sensing bacterial colonizers. Proc. Natl. Acad. Sci. U. S. A 109, 19374–19379. https://doi.org/10.1073/pnas.1213110109.

Fuess, L.E., Pinzón C, J.H., Weil, E., Grinshpon, R.D., Mydlarz, L.D., 2017. Life or death: disease-tolerant coral species activate autophagy following immune challenge. Proc. R. Soc. B 284, 20170771. https://doi.org/10.1098/rspb.2017.0771.

Fuess, L.E., Pinzón C, J.H., Weil, E., Mydlarz, L.D., 2016. Associations between transcriptional changes and protein phenotypes provide insights into immune regulation in corals. Dev. Comp. Immunol. 62, 17–28. https://doi.org/10.1016/j.dci.2016.04.017.

Garbati, M.R., Alço, G., Gilmore, T.D., 2010. Histone acetyltransferase p300 is a coactivator for transcription factor REL and is C-terminally truncated in the human diffuse large B-cell lymphoma cell line RC-K8. Cancer Lett. 291, 237–245. https://doi.org/10.1016/j.canlet.2009.10.018.

Gauthier, M.E.A., Du Pasquier, L., Degnan, B.M., 2010. The genome of the sponge *Amphimedon queenslandica* provides new perspectives into the origin of Toll-like and interleukin 1 receptor pathways. Evol. Dev. 12, 519–533. https://doi.org/10.1111/j.1525-142X.2010.00436.x.

Gilmore, T.D., 2006. Introduction to NF-κB: players, pathways, perspectives. Oncogene 25, 6680–6684. https://doi.org/10.1038/sj.onc.1209954.

Gilmore, T.D., Wolenski, F.S., 2012. NF-κB: where did it come from and why? Immunol. Rev. 246, 14–35. https://doi.org/10.1111/j.1600-065X.2012.01096.x.

Gleason, D.F., Wellington, G.M., 1993. Ultraviolet radiation and coral bleaching. Nature 365, 836–838. https://doi.org/10.1038/365836a0.

Hayden, M.S., Ghosh, S., 2004. Signaling to NF-κB. Genes Dev. 18, 2195–2224. https://doi.org/10.1101/gad.1228704.

Hoegh-Guldberg, O., Mumby, P.J., Hooten, A.J., Steneck, R.S., Greenfield, P., Gomez, E., Harvell, C.D., Sale, P.F., Edwards, A.J., Caldeira, K., Knowlton, N., Eakin, C.M., Iglesias-Prieto, R., Muthiga, N., Bradbury, R.H., Dubi, A., Hatziolos, M.E., 2007. Coral reefs under rapid climate change and ocean acidification. Science 318, 1737–1742. https://doi.org/10.1126/science.1152509.

Hughes, T.P., Kerry, J.T., Álvarez-Noriega, M., Álvarez-Romero, J.G., Anderson, K.D., Baird, A.H., Babcock, R.C., Beger, M., Bellwood, D.R., Berkelmans, R., Bridge, T.C., Butler, I.R., Byrne, M., Cantin, N.E., Comeau, S., Connolly, S.R., Cumming, G.S., Dalton, S.J., Diaz-Pulido, G., Eakin, C.M., Figueira, W.F., Gilmour, J.P., Harrison, H.B., Heron, S.F., Hoey, A.S., Hobbs, J.-P.A., Hoogenboom, M.O., Kennedy, E.V., Kuo, C.-Y., Lough, J.M., Lowe, R.J., Liu, G., McCulloch, M.T., Malcolm, H.A., McWilliam, M.J., Pandolfi, J.M., Pears, R.J., Pratchett, M.S., Schoepf, V., Simpson, T., Skirving, W.J., Sommer, B., Torda, G., Wachenfeld, D.R., Willis, B.L., Wilson, S.K., 2017. Global warming and recurrent mass bleaching of

corals. Nature 543, 373–377. https://doi.org/10.1038/nature21707.
Kawai, T., Akira, S., 2007. Signaling to NF-κB by toll-like receptors. Trends Mol. Med. 13, 460–469. https://doi.org/10.1016/j.molmed.2007.09.002.
Kushmaro, A., Loya, Y., Fine, M., Rosenberg, E., 1996. Bacterial infection and coral bleaching. Nature 380. https://doi.org/10.1038/380396a0, 396–396.
Mansfield, K.M., Carter, N.M., Nguyen, L., Cleves, P.A., Alshanbayeva, A., Williams, L.M., Crowder, C., Penvose, A.R., Finnerty, J.R., Weis, V.M., Siggers, T.W., Gilmore, T.D., 2017. Transcription factor NF-κB is modulated by symbiotic status in a sea anemone model of cnidarian bleaching. Sci. Rep. (in press).
Miller, D.J., Hemmrich, G., Ball, E.E., Hayward, D.C., Khalturin, K., Funayama, N., Agata, K., Bosch, T.C.G., 2007. The innate immune repertoire in cnidaria–ancestral complexity and stochastic gene loss. Genome Biol. 8 https://doi.org/10.1186/gb-2007-8-4-r59. R59.
Minakhina, S., Steward, R., 2006. Nuclear factor-kappa B pathways in *Drosophila*. Oncogene 25, 6749–6757. https://doi.org/10.1038/sj.onc.1209940.
O'Neill, L.A.J., Dunne, A., Edjeback, M., Gray, P., Jefferies, C., Wietek, C., 2003. Mal and MyD88: adapter proteins involved in signal transduction by Toll-like receptors. J. Endotoxin Res. 9, 55–59. https://doi.org/10.1179/096805103125001351.
Pinzón, J.H., Kamel, B., Burge, C.A., Harvell, C.D., Medina, M., Weil, E., Mydlarz, L.D., 2015. Whole transcriptome analysis reveals changes in expression of immune-related genes during and after bleaching in a reef-building coral. R. Soc. Open Sci. 2, 140214. https://doi.org/10.1098/rsos.140214.
Poole, A.Z., Weis, V.M., 2014. TIR-domain-containing protein repertoire of nine anthozoan species reveals coral-specific expansions and uncharacterized proteins. Dev. Comp. Immunol. 46, 480–488. https://doi.org/10.1016/j.dci.2014.06.002.
Shinzato, C., Shoguchi, E., Kawashima, T., Hamada, M., Hisata, K., Tanaka, M., Fujie, M., Fujiwara, M., Koyanagi, R., Ikuta, T., Fujiyama, A., Miller, D.J., Satoh, N., 2011. Using the *Acropora digitifera* genome to understand coral responses to environmental change. Nature 476, 320–323. https://doi.org/10.1038/nature10249.
Sievers, F., Wilm, A., Dineen, D., Gibson, T.J., Karplus, K., Li, W., Lopez, R., McWilliam, H., Remmert, M., Söding, J., Thompson, J.D., Higgins, D.G., 2011. Fast, scalable generation of high-quality protein multiple sequence alignments using clustal omega. Mol. Syst. Biol. 7, 539. https://doi.org/10.1038/msb.2011.75.
Siggers, T., Chang, A.B., Teixeira, A., Wong, D., Williams, K.J., Ahmed, B., Ragoussis, J., Udalova, I.A., Smale, S.T., Bulyk, M.L., 2011. Principles of dimer-specific gene regulation revealed by a comprehensive characterization of NF-κB family DNA binding. Nat. Immunol. 13, 95–102. https://doi.org/10.1038/ni.2151.
Silverman, N., Maniatis, T., 2001. NF-κB signaling pathways in mammalian and insect innate immunity. Genes Dev. 15, 2321–2342. https://doi.org/10.1101/gad.909001.
Starczynowski, D.T., Trautmann, H., Pott, C., Harder, L., Arnold, N., Leeman, J.R., Siebert, R., Gilmore, T.D., 2007. Mutation of an IKK phosphorylation site within the transactivation domain of REL in two patients with B-cell lymphoma enhances REL's *in vitro* transforming activity. Oncogene 26, 2685–2694. https://doi.org/10.1038/sj.onc.1210089.
Steele, R.E., David, C.N., Technau, U., 2011. A genomic view of 500 million years of cnidarian evolution. Trends Genet. 27, 7–13. https://doi.org/10.1016/j.tig.2010.10.002.
Stöven, S., Silverman, N., Junell, A., Hedengren-Olcott, M., Erturk, D., Engström, Y., Maniatis, T., Hultmark, D., 2003. Caspase-mediated processing of the *Drosophila* NF-κB factor relish. Proc. Natl. Acad. Sci. U.S.A. 100, 5991–5996. https://doi.org/10.1073/pnas.1035902100.
Sullivan, J.C., Kalaitzidis, D., Gilmore, T.D., Finnerty, J.R., 2007. Rel homology domain-containing transcription factors in the cnidarian *Nematostella vectensis*. Dev. Genes Evol. 217, 63–72. https://doi.org/10-1007/s00427-006-0111-6.
Sullivan, J.C., Wolenski, F.S., Reitzel, A.M., French, C.E., Traylor-Knowles, N., Gilmore, T.D., Finnerty, J.R., 2009. Two alleles of NF-κB in the sea anemone *Nematostella vectensis* are widely dispersed in nature and encode proteins with distinct activities. PloS One 4, e7311. https://doi.org/10.1371/journal.pone.0007311.
Sun, S.-C., 2011. Non-canonical NF-κB signaling pathway. Cell Res. 21, 71–85. https://doi.org/10.1038/cr.2010.177.
Swofford, D.L., 2001. PAUP*: Phylogenetic Analysis Using Parsimony (And Other Methods) Version 4.0.B5. Sinauer Associates, Sunderland, MA.
Valanne, S., Wang, J.-H., Rämet, M., 2011. The *Drosophila* Toll signaling pathway. J. Immunol. 186, 649–656. https://doi.org/10.4049/jimmunol.1002302.
Vasselon, T., Detmers, P.A., 2002. Toll receptors: a central element in innate immune responses. Infect. Immun. 70, 1033–1041. https://doi.org/10.1128/IAI.70.3.1033-1041.2002.
Weis, V.M., 2008. Cellular mechanisms of Cnidarian bleaching: stress causes the collapse of symbiosis. J. Exp. Biol. 211, 3059–3066. https://doi.org/10.1242/jeb.009597.
Wolenski, F.S., Garbati, M.R., Lubinski, T.J., Traylor-Knowles, N., Dresselhaus, E., Stefanik, D.J., Goucher, H., Finnerty, J.R., Gilmore, T.D., Mar 2011. Characterization of the core elements of the NF-κB signaling pathway of the sea anemone *Nematostella vectensis*. Mol. Cell. Biol. 31, 1076–1087. https://doi.org/10.1128/MCB.00927-10.
Wolenski, F.S., Layden, M.J., Martindale, M.Q., Gilmore, T.D., Finnerty, J.R., 2013. Characterizing the spatiotemporal expression of RNAs and proteins in the starlet sea anemone, *Nematostella vectensis*. Nat. Protoc. 8, 900–915. https://doi.org/10.1038/nprot.2013.014.
Zhou, Z., Wu, Y., Zhang, C., Li, C., Chen, G., Yu, X., Shi, X., Xu, Y., Wang, L., Huang, B., 2017. Suppression of NF-κB signal pathway by NLRC3-like protein in stony coral *Acropora aculeus* under heat stress. Fish. Shellfish Immunol. 67, 322–330. https://doi.org/10.1016/j.fsi.2017.06.027.